Biomedicine & Pharmacotherapy 164 (2023) 114984

Contents lists available at ScienceDirect

Biomedicine & Pharmacotherapy

journal homepage: www.elsevier.com/locate/biopha

Antileishmanial, cellular mechanisms, and cytotoxic effects of green synthesized zinc nanoparticles alone and in combined with glucantime against *Leishmania major* infection

Javad Ghasemian Yadegari [a], Amal Khudair Khalaf [f], Fatemeh Ezzatkhah [b], Mojtaba Shakibaie [c], Hamid Reza Mohammadi [a], Hossein Mahmoudvand [d,e,*]

[a] Department of Pharmacognosy, School of Pharmacy, Lorestan University of Medical Sciences, Khorramabad, Iran
[b] Department of Laboratory Sciences, Sirjan School of Medical Sciences, Sirjan, Iran
[c] Pharmaceutical Sciences and Cosmetic Products Research Center, Kerman University of Medical Sciences, Kerman, Iran
[d] Razi Herbal Medicines Research Center, Lorestan University of Medical Sciences, Khorramabad, Iran
[e] Molecular and Cellular Laboratory, School of Allied Medicine, Lorestan University of Medical Sciences, Khorramabad, Iran
[f] Department of Microbiology, College of Medicine, University of Thiqar, Iraq

ARTICLE INFO

Keywords:
Leishmania
Amastigote
Nitric oxide
Lesion
Nanoparticles

ABSTRACT

Background: We decided to investigate the antileishmanial, cellular mechanisms, and cytotoxic effects of green synthesized Zinc nanoparticles (ZnNPs) alone and combined with glucantime against *Leishmania major* infection.
Methods: The effect of green synthesized ZnNP on *L. major* amastigote was studied through macrophage cells. The mRNA expression level of iNOS and IFN-γ followed by the exposure of J774-A1 macrophage cells to ZnNPs was assessed by Real-time PCR. The Caspase-3-like activity of promastigotes exposed to ZnNPs was studied. Effects of ZnNPs alone and combined with glucantime (MA) were studied on cutaneous leishmaniasis in BALB/c mice.
Results: ZnNPs displayed the spherical shape with sizes ranging from 30 to 80 nm. The obtained IC_{50} values for ZnNPs, MA, and ZnNPs + MA were 43.2, 26.3, and 12.6 μg/mL, respectively; indicating the synergistic effects of ZnNPs in combination with MA. CL lesions had completely improved in the mice received with ZnNPs in combination with MA. The mRNA expression level of iNOS, TNF-α, and IFN-γ was dose-dependently ($p < 0.01$) upregulated; whereas it was downregulated in IL-10. ZnNPs markedly stimulated the caspase-3 activation with no significant toxicity on normal cells.
Conclusion: Based on these in vitro and in vivo results, green synthesized ZnNPs, mainly along with MA, showed that has the potential to be introduced as a new drug for CL therapy. Triggering of NO production, and inhibition of infectivity rate are revealed as mechanisms of action ZnNPs on *L. major*. But, supplementary investigations are necessary to clear the efficacy and safety of these agents.

1. Introduction

Leishmaniasis is one of the important parasitic diseases, that spreads in different tropical and subtropical regions of the world including Iran [1]. The World Health Organization has estimated the number of people at risk at 350 million and the number of people infected with the disease at 12 million, to which more than 1,500,000 new cases are added every year [1,2]. Over time, various methods including local radiation therapy, burning the lesion site, cryotherapy, and local infiltration of drugs have been used to treat cutaneous leishmaniasis (CL) [3]. Currently, for the treatment of cutaneous leishmaniasis, pentavalent antimony compounds such as pentostam (sodium stibogluconate) and glucantime (meglumine antimonate) are considered the first-line drugs for the treatment of this disease [4]. The use of these compounds has limitations such as long treatment periods, expensive drugs, lack of treatment response in about 10–15 % of cases, and severe toxicity on the heart, liver, and kidneys [5,6]. Therefore, extensive research is currently being done on leishmaniasis treatment methods.

Nanotechnology is the application of science to control substances at the molecular level [7]. Nanotechnology plays a very important role in

Abbreviations: ZnNPs, Zinc nanoparticles; CL, cutaneous leishmaniasis; IC_{50}, 50 % inhibitory concentrations; SI, selectivity index.

* Corresponding author at: Razi Herbal Medicines Research Center, Lorestan University of Medical Sciences, Khorramabad, Iran.
E-mail address: dmahmodvand@gmail.com (H. Mahmoudvand).

https://doi.org/10.1016/j.biopha.2023.114984
Received 22 March 2023; Received in revised form 30 May 2023; Accepted 1 June 2023
Available online 13 June 2023
0753-3322/© 2023 The Authors. Published by Elsevier Masson SAS. This is an open access article under the CC BY license (http://creativecommons.org/licenses/by/4.0/).

modern research and is the most powerful technology that can be used in all fields such as pharmacology, electronics, health, food and nutrition, biomedical science, medicine and gene transfer, chemical industry, energy science, cosmetics, health environment, mechanics and space industries, it is also used to treat diseases, cancer, allergies, diabetes and inflammation [8]. The synthesis of metal nanoparticles using plant extracts is an economical method. The plant extracts for the synthesis of nanoparticles can have two reducing and protective roles at the same time [9,10].

Zinc (Zn) is the second most common element in the human body, which plays a role in the activation of more than 300 enzymes that regulate the biosynthesis of macromolecules in DNA, RNA, protein, as well as cell growth and proliferation, and other types of metabolism [11]. It is vital for human health, so its deficiency leads to reduced growth, lack of appetite, impaired immune system, increased oxidative stress, skin reactions, delayed wounds, and reduced reproductive capacity [12]. Zinc (Zn) affects the production of anti-inflammatory cytokines such as interleukin-1β, IL-6, and TNF-α. This element is also involved in identifying NK cells from MHC class 1 main cells. Zn is also very important for the balance between different subsets of T cells [13].

Zinc nanoparticles (ZnNPs) are also one of the widely used nanoparticles that have suitable physical and chemical properties, which can be attributed to high chemical stability, low dielectric constant, high catalytic activity, and absorption of infrared and ultraviolet light [14,15]. According to the previous studies that show the antimicrobial activity and effects of these nanoparticles, and taking into account the fact that no documented study has been done on the anti-leishmanial activity of zinc nanoparticles synthesized with lavender plant on *Leishmania* species. We decided to investigate the anti-leishmanial effects of ZnNPs green synthesized by lavender (*Lavandula angustifolia* Vera.), a herb from the family Lamiaceae with a broad spectrum of biological and therapeutic features, e.g., antimicrobial, antioxidant, and anti-inflammatory [16], by microwave method.

2. Materials and methods

2.1. Chemicals

Fetal calf serum, Dulbecco's modified Eagle's medium (DMEM), RPMI 1640, ZnSO4 solution, Griess reagents, and MTT powder ([3-(4.5-dimethylthiazol-2-yl)-2.5-diphenyl tetrazolium bromide)]) were procured from Sigma-Aldrich, Germany. All other materials were purchased with the best quality.

2.2. Plant preparation and extraction

The leaves of lavender were collected from the rural areas of Kerman in the spring of 2022 and after the confirmation and identification of the plant by a botanist (Voucher no. 2627), they were transferred to the laboratory and dried and turned into powder using an electric grinder. In the next step, 300 g of the resulting powder is dissolved in a solution of water and alcohol in equal proportions (50 % water and 50 % alcohol) and placed at room temperature for 24 h. Since alcohol separates more substances and both polar and non-polar compounds than other solvents, absolute ethanol alcohol was used in this study. After filtering the obtained solution, the solvent (water and alcohol) is evaporated by the rotary evaporator device and then the remaining material is dried and turned into a powder which will be used as a hydroalcoholic extract [17,18].

2.3. Secondary metabolites analysis of the extract

Folin-Ciocalteu's method was considered to determine the total content of phenolic compounds based on the methods described elsewhere [19]. Briefly, in this method, 20 μL of the extract was mixed with distilled water and 100 μL of Folin Ciocalteu reagent. After adding sodium carbonate solution (20 %, 300 μL) to the test tube. The absorbance of tubes was measured with a spectrophotometer at a wavelength of 760 nm. The results were expressed in terms of milligrams of gallic acid per gram of extract. Aluminum chloride (AlCl3) colorimetric was also used to assess the total flavonoid content of the extract based on the methods explained previously [20]. Briefly, followed by mixing the extract, AlCl3 (0.1 %), potassium acetate (0.1 %), ethanol (95 %), and distilled water, the mixture was kept at 21 C0 for 30 min. The absorbance of the combination was recorded at 415 nm. The results were expressed in terms of milligrams of quercetin per gram of extract.

2.4. Green synthesis of ZnNPs

ZnNP was green synthesized according to the method described by Salari et al. [21]. At first, 10 mL of lavender extract (5 mg/mL) was mixed with $ZnSO_4$ solution (40 mL) in a reaction vessel by passing pure argon into the solution. Then, the reaction combination was exposed to a microwave oven (850 W) for the 60 s to decline the ions of Zn. The combination was stirred outside the oven at 21 °C for 10 min and the mentioned procedures were repeated three times. The appearance of a dark gray color is considered a provisional marker for the synthesis of Zn NPs. The nanoparticles were separated by centrifugation at 12,000 rpm, for 30 min and the separated ZnNPs were then washed with chloroform, ethyl alcohol, and distilled water, respectively, and characterized using different techniques.

3. Characterization of biogenic ZnNPs

3.1. UV–Vis spectrum analysis

A spectrophotometer (JENWAY 6405) was applied for determining the UV–visible. In addition, and X-ray diffractometer (Philips, PW1710) prepared with CuK emission in the 2θ varying from 0 to 80o was used to identify the crystalline construction of Zn NPs.

3.2. Scanning electron microscope (SEM) analysis

The surface and basic construction of the Zn NPs were detected through the SEM device (KYKY-EM3200) provided with X-ray (EDX) microanalyzer,

3.3. Fourier transform infrared spectroscopy

The ZnNPs surface chemistry was identified using FTIR spectrophotometer (Shimadzu IR-470, Japan) with 40 mm resolution in the potassium bromide records.

3.4. Parasite and cell culture

L. major parasites (promastigote, MRHO/IR/75/ER) were cultured in RPMI 1640 upgraded with 10 % FCS and penicillin/streptomycin (100 μg/mL). Macrophage cells (J774-A1) were cultured in DMEM enhanced with 20 % FCS at 37 °C in 5 % CO_2.

3.5. Effect of ZnNPs on amastigote forms

Firstly, 100 μL of macrophage cells (1×10^5/mL) was added to 24-wells plate with rounded coverslips on the, floor and then plates were incubated overnight at 37 °C in 5 % CO_2. In the next step, 100 μL of *L. major* promastigotes (1×10^6/mL) in stationary phase (at ratio of 10:1) were added to the wells and then were incubated at 37 °C in 5 % CO_2 for 24 h. Different concentrations of ZnNPs and glucantime (3.125–50 μg/mL) were distinctly added to each well comprising infected macrophage cells for 48 h. As a final point, slides were fixed in absolute methanol, stained with Giemsa dye, and studied under light microscopy. The number of amastigotes forms in 100 macrophages was

Table 1
The primers applied for real-time PCR.

Amplicon	Primers	Sequence (5′–3′)
iNOS	F	TGCCGGAAGGCGGCTCATTC
	R	CGCAGTGCGTTGCGCATACC
IFN-γ	F	TGCCGGAAGGCGGCTCATTC CGCAGTGCGTTGCGCATACC
	R	
IL-10	F	CACTCCCAAAACCTGCTGAG
	R	TCTCTTCAGAAGTGCAAGGGTA
TNF-α	F	AGTTCCCAAATGGCCTCCCTCTCA
	R	GTGGTTTGCTACGACGTGGGCT
β-actin	F	GTGACGTTGACATCCGTAAAGA
	R	GCCGGACTCATCGTACTCC

recorded and the 50 % inhibitory concentrations (IC_{50}) were determined by using the Probit test in SPSS software (Ver. 26.0). The examinations were carried out in triplicate and the findings were indicated as mean ± standard deviation [22].

3.6. Fractional inhibitory concentration index

The synergistic effects of ZnNPs in combination with MA, we determined the Fractional inhibitory concentration index (FICI) through the following formula:

FICI = IC_{50} in combination/IC_{50} drug alone

The results are interpreted as FICI ≤ 0.5 showed the synergistic effects; whereas 0.5 < FICI < 1 and FICI < 4 showed the additive and antagonistic effects, respectively [23].

3.7. Effect of extract on the infectivity rate in macrophages

For performing this test, *L. major* promastigotes (1×10^6/mL) were pre-treated with ZnNPs (IC_{50}) for two hours at 21 °C. The treated promastigotes were washed and again exposed to macrophage cells for 24 h. Finally, the slides were prepared and stained with Giemsa dye and were examined under a light microscope by calculating 100 cells [24].

3.8. Effect of extract on nitric oxide (NO) production

After incubating the J774-A1 macrophage cells (1×10^5/mL) with chloroform extract of ZnNPs at 1/4 IC_{50}, 1/3 IC_{50}, and ½ IC_{50} for 48 h, the collected supernatants (100 μL) were transferred to a 96-well microplate. Then, 50 μL of the Griess reagent A and B were added to the tested wells. The absorbance of microplates was measured at 540 nm in an ELISA reader [22]. The cells treated with the combination of lipopolysaccharide (10 ng/mL) along with IFN-γ (10 U/mL) were considered as the positive control.

3.9. The mRNA expression level of iNOS and proinflammatory cytokines IFN-γ

Followed by the exposure of J774-A1 macrophage cells (1×10^5/mL) with ZnNPs at 1/3 IC50, ½ IC50, and IC_{50} for 48 h, the collected supernatants (100 μL) were transferred to a 96-well microplate. Total RNA was extracted according to the commercial kit protocols (Yekta Tajhiz, Iran). The extracted RNAs were then reverse-transcribed based on the commercial kit (Fermentas, USA). All amplification products were assessed by SYBR green Real-time PCR [25] for evaluation of the expression level of interferon-gamma (IFN-γ) and interleukin 10 (IL-10), tumor necrosis factor-alpha (TNF-α), and inducible nitric oxide synthase (iNOS). The thermal conditions were performed with primary denaturation at 94 °C for 12 min, 40 amplification cycles [denaturation at 94 °C for 10 s, annealing at 55 °C for 30 s, and elongation at 70 °C for 30 s], next a single cycle at 70 °C for 5 min. Finally, ΔΔCt-2 was calculated using CA, Hercules, Rad-Bio optical system software (iQTM5) and β-actin was applied to normalize the mRNA levels of tested samples. The sequence of primers used for real-time PCR is shown in Table 1.

3.10. Caspase-3-like activity of ZnNPs-treated parasites

The Caspase-3-like activity of promastigotes exposed with ZnNPs was studied by using the Caspase-3 Colorimetric Activity Assay Kits (Sigma-Aldrich, Darmstadt, Germany) according to the manufacturer protocol. Briefly, parasites 1×10^6 were exposed to ZnNPs at 1/3 IC_{50}, 1/2 IC_{50}, and IC_{50} for 48 h. Then, the mixture was centrifuged at 600 rpm for 10 min at 4 °C. The collected cell remains were lysed, and the cell lysate was centrifuged again at 15,000 rpm for 10 min. Next 5 μL of the upper phase of the combination was mixed to buffer (85 μL) and caspase-3 solution (10 μL) and incubated at 37 °C for 2 h. The light absorbance of the mixture at 405 nm was recorded by an ELISA reader [26].

3.11. Cytotoxic effects of J774-A1 macrophage cells

To do this, 100 μL of macrophage cells (1×10^5/mL) were added to each 96-well plate, and various concentrations of ZnNPs (50–800 μg/mL) were separately added to each well containing the macrophages and incubated at 24 °C for 48 and 72 h. Then, 10 μL of MTT solution (5 mg/mL) was added to each well and kept in the incubator for 4 h; 150 microliters of DMSO was added to each of the wells, and after 30 min, the absorption of the cells was read by the ELISA reader in the absorption wavelength of 570 nm. The 50 % cytotoxic concentrations (CC_{50}) values were evaluated using the Probit test in SPSS software (Ver. 26.0). Also, to study cytotoxicity and efficacy of extract, the selectivity index (SI) was measured based on the equation CC_{50} /IC_{50} for amastigotes [23].

3.12. The selectivity index (SI) measurement

The SI of ZnNPs was measured by dividing the CC_{50} value of macrophage cells on IC_{50} vale of amastigote forms; whereas SI value more than 10, indicates promising antileishmanial effects of ZnNPs on intracellular amastigotes with no cytotoxic effects on host macrophage cells [24].

4. Effect of ZnNPs on CL in mice

4.1. Animals

A total of 56 male BALB/c mice (seven groups containing eight mice per each) at 40–60 days old (25–30 g) were reserved in a colony room (21 ± 2 °C) with a 12-h/2-h light/dark cycle; whereas, each group of the tested mice was kept in a separated cage (CT2. PN, Tajhizgostar, Iran).

4.2. Establishing the animal model

CL was established through the subcutaneous inoculation of 0.1 mL of promastigotes (1×10^6 cells/mL) in the stationary stage at the base of the mice's tail [26].

4.3. Treating of CL in mice

Treatment of infected mice starts 42 days after parasite inoculation and when CL appeared. Treatment groups were included:

I: CL mice treated with normal saline.

II: CL mice treated with intralesional administration MA (12.5 mg/kg).

III: CL mice treated with intralesional administration MA (25 mg/kg).

IV: CL mice topically treated with ZnNPs at 10 mg/kg/day for 28 day.

V: CL mice topically treated with ZnNPs at 20 mg/kg/day for 28 day.

Table 2
Antileishmanial and cytotoxic effects of green synthesized zinc nanoparticles (ZnNPS), and glucantime (MA) by determining 50 % inhibitory concentrations (IC50), 50 % cytotoxic concentrations (CC50), selectivity index (SI), and fractional inhibitory concentration index (FICI). Mean ± standard deviation. (n = 3).

Drug	IC50 (μg/mL) Amastigote	CC_{50} (μg/mL)	SI	FICI
ZnNPs	43.2 ± 3.12	612.3 ± 11.25	14.2	0.29
MA	23.3 ± 2.14	784.6 ± 14.2	33.6	0.48
ZnNPs + MA	12.6 ± 0.73	328.4 ± 14.2	26.1	-

VI: CL mice topically treated with ZnNPs at 10 mg/kg/day for 28 day+ MA (25 mg/kg).

VII: CL mice topically treated with ZnNPs at 10 mg/kg/day for 28 day+ MA (12.5 mg/kg).

4.4. Evaluation of antileishmanial effects of ZnNPs on CL in mice

Followed by 28 days' treatment, the size of CL lesions in mice was recorded by a Vernier caliper before and after treatment. Additionally, the parasite load was calculated by impression smears gained from the wounds. The smears were firstly fixed with methanol and, next stained with Giemsa, and were checked with a light microscope [26].

4.5. Quantification of parasite load in liver

Parasite burden in liver tissue was determined based on the limiting dilution assay (LDA) according to the method described elsewhere [27]. After the treatment of the mice was over, the liver and spleen tissues were aseptically collected, weighed, and then homogenized in 2 mL Schneider's medium (Sigma-Aldrich, Germany) enhanced with 20 % FCS, and penicillin/streptomycin (100 μg/mL). After preparing the serial dilutions of tissue homogenates in quadruplicate in sterile flat-bottom-96 well plates, they were incubated at 25 ± 1 °C for 10 days. The motile and non-motile parasites were assessed with an inverted microscope. The mean number of viable parasites per mg of tissue was recorded by the highest dilution at which growing promastigotes using ELIDA software.

4.6. Determining the proinflammatory cytokines

Analysis of the proinflammatory cytokines (IFN-γ, TNF-α, and IL-1) in the serum of mice treated with ZnNPs was performed based on commercial Enzyme-linked immunosorbent assay (ELISA) kits (Karmania Pars Gene, Iran) based on the producer protocols.

4.7. Statistical analysis

To compare the anti-leishmanial effects of zinc nanoparticles in different concentrations, ANOVA and Tukey's tracking test were used. Also, to determine the anti-parasitic effects of different concentrations of ZnNPs compared to the control group, analysis of variance and Dent's post hoc test were used. All statistical tests were performed using SPSS version 25 software (IBM, U.S.A), and $P < 0.05$ was considered as the significance level.

5. Results and discussion

Analysis of the total phenolic and flavonoid contents of *L. vera* extract showed that the total phenolic and flavonoid content was 691 (mg GEA/g DW) and 91.8 (mg QE/g DW) respectively. The synthesis ZnNPs was confirmed by UV–VIS analysis with absorption peaks ranging from 230 to 330 nm. EDX results also revealed that Zn adsorption peaks were $ZnL\alpha_1$, $ZnK\alpha_1$, and $ZnK\beta_1$ were 1.01, 8.64, and 9.57 kg, respectively. By XRD patterns, peaks of 101–300 were refractive peaks at 19.6–54.8 degrees. The obtained peaks in FTIR (e.g., 1401, 1262, 1064, and 580 cm) were probably linked to CC, CN, CN, and C- (F, Cl or BR); where, the maximum adsorption at 1627 cm, 3418 cm and 2923 cm were linked to the polypeptide amide Bond-1, OH stretching. The findings of the SEM also revealed that spherical shape ZnNPs with sizes ranging from 30 to 80 nm, whereas the majority of them were between 50 and 60 nm (Suppl.1).

The results of the macrophage model showed that the number of amastigotes significantly declined after treatment of infected macrophages with ZnNPs mainly in combination with MA ($P < 0.001$). The obtained IC_{50} values for ZnNPs, MA, and ZnNPs + MA were 43.2, 26.3, and 12.6 μg/mL, respectively (Table 2). The calculated FICI value for ZnNPs and MA was 0.29 and 0.48, respectively; indicating the

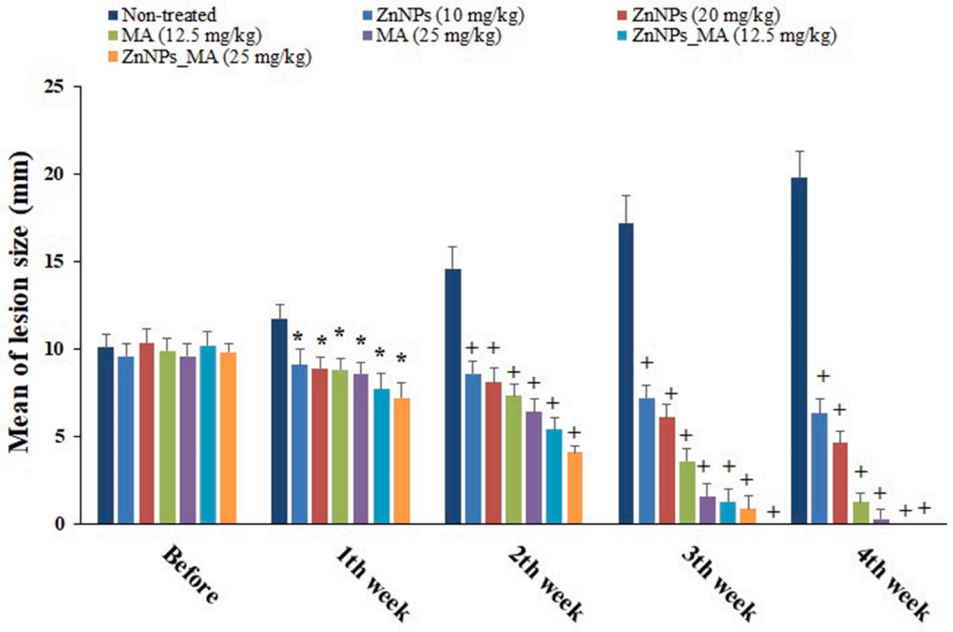

Fig. 1. Effect of various concentrations of the green synthesized zinc nanoparticles (ZnNPs) alone and in combined with meglumine antimoniate (MA) on the lesions size in BALB/c mice infected by *L. major*. Mean ± standard deviation. * $p < 0.05$ and + $p < 0.001$.

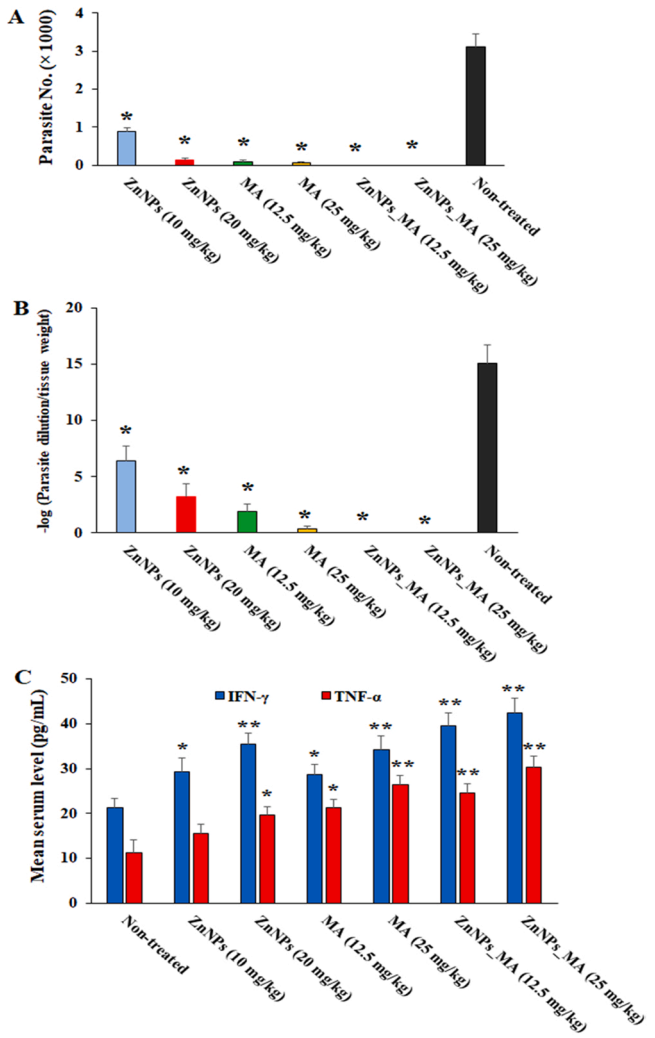

Fig. 2. Effect of various concentrations of the green synthesized zinc nanoparticles (ZnNPs) alone and in combined with meglumine antimoniate (MA) the mean number of parasites (parasite load) in lesion (A) and liver tissue (B) as well as the serum level of IFN-γ and TNF-α in BALB/c mice infected by *L. major* (C). Mean ± standard deviation. * $p < 0.05$ and ** $p < 0.001$.

synergistic effects of ZnNPs in combination with MA. The results of in vivo revealed that the treatment of infected mice with ZnNPs alone and in combination with MA reduced the diameter of CL lesions; whereas, after 28 days' treatment, CL lesions had completely improved in the mice received with ZnNPs (10 mg/kg) in combination with MA (25 mg/kg) (Fig. 1). The parasite number in the lesion was also significantly reduced ($p < 0.001$) followed by treatment of the infected mice with ZnNPs especially in combination with MA (Fig. 2A). As shown in Fig. 2B, the parasite burden liver tissue was markedly ($P < 0.001$) declined followed by treatment of the infected mice with ZnNPs especially in combination with MA. After 28 days treatment with ZnNPs, the serum level of proinflammatory cytokines of IFN-γ and TNF-α was dose-dependently increased ($P < 0.01$) (Fig. 2C). Previous studies revealed that nano-drug delivery systems via elevating bioavailability, dropping toxicity, aggregating the concentration, and extending systemic circulation lifetime, enhanced the effectiveness of conventional agents [28,29].

Inhibition infection in host cells by these drugs is well-known as one of the main factors in the evaluation of the effect of new agents on *Leishmania* pathogenesis [29]. By microscopic results, the results demonstrated that the percent of non-treated infected macrophages by no pre-treated promastigotes was 79.4 ± 2.73. We found that

Table 3
Infection inhibition of the in macrophage cells followed by pre-treatment of promastigotes with green synthesized ZnNPs at ¼ IC50, 1/3 IC50, 1/2 IC50. mean ± SD.

Treatment	% of infected macrophages	% of reduction
¼ IC_{50}	70.5 ± 6.12	11.2
1/3 IC_{50}	57.5 ± 5.3	27.6
1/2 IC_{50}	41.1 ± 3.15	48.3*
Non-treated	79.4 ± 2.73	-

* $p < 0.05$.

Table 4
The effect of green synthesized zinc nanoparticles (ZnNPs) on nitric oxide (NO) generation in J774-A1 macrophages cells in comparison with the control groups. Mean ± SD.

Material	NO production (nM)
¼ IC_{50}	4.23 ± 0.37
1/3 IC_{50}	5.12 ± 0.65*
1/2 IC_{50}	11.2 ± 1.62*
Non-treated	3.21 ± 0.56
IFN-γ + LPS	27.8 ± 3.51

* $p < 0.001$.

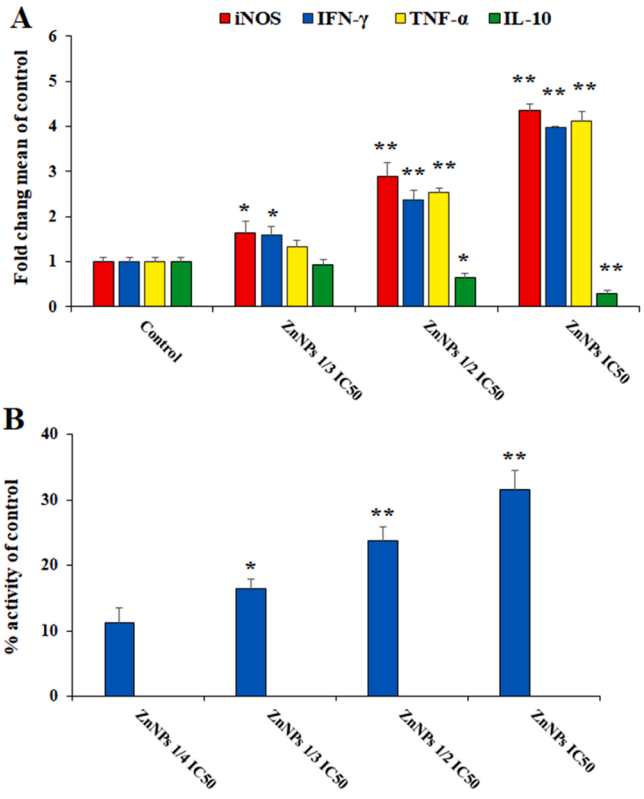

Fig. 3. The mRNA expression level of iNOS and IFN-γ followed by the exposure of J774-A1 macrophage cells with green synthesized zinc nanoparticles (ZnNPs) at 1/3 IC50, ½ IC50, and IC_{50} for 48 h (A); the Caspase-3 activity of parasites exposed with ZnNPs at ¼ IC50, 1/3 IC50, ½ IC50, and IC50 for 48 h (B). * $p < 0.05$ shows the difference was statistically significant in comparison with control. Mean ± standard deviation.

pre-treatment of parasites with the ZnNPs at ¼ IC_{50}, 1/3 IC_{50}, and 1/2 IC_{50} reduced the rate of macrophage infection by 11.2 %, 27.6 %, and 48.3 %, respectively (Table 3). NO is well-known as a main factor involved in innate immunity to control and eliminate intracellular parasites such as *Leishmania* spp [30,31]. IFN-γ also plays critical role in

the progress and subsequent control of leishmaniasis [30,31]. Based on the results of the Griess reagent assay, the macrophages treated with ZnNPs triggered the NO release, nevertheless a significant ($p < 0.001$) increase was indicated at ½ IC_{50} compared to the control group (Table 4). Followed by the exposure of the macrophages with FO, the NO release was increased, however, a significant ($p < 0.05$) rise was reported at 1/3 IC50 and ½ IC50 compared to the control group with NO production values of 4.24 ± 0.85 and 12.3 ± 1.42 nM, respectively. While the rate of NO production for non-treated cells and cells treated with IFN-γ + LPS was 2.49 ± 0.31 and 30.24 ± 4.45 nM, respectively (Table 2). Real-time PCR also indicated that followed by the exposure of the macrophages with ZnNPs at 1/3 IC_{50}, ½ IC_{50}, and IC_{50} for 48 h, the mRNA expression level of iNOS, IFN-γ, and TNF-α was dose-dependently ($p < 0.01$) upregulated as the dose-dependent manner (Fig. 3A); whereas, the mRNA expression level of IL-10 was dose-dependently ($p < 0.01$) downregulated. Apoptosis is considered a key process that links an organism's endurance to its capacity to induce cell death [32]. Caspases are the main mediators of this process; whereas, Caspase-3 is well-known as the chief caspase which generally triggers death protease and successively provoke cell death [33]. In recent decades, apoptosis induction is judged as one of the key promising antimicrobial mechanisms of tested drugs, therefore, we tested the Caspase-3-like activity of parasites exposed to ZnNPs. The results obviously reflected that the ZnNPs at ¼ IC_{50}, 1/3 IC_{50}, 1/2 IC_{50}, and IC_{50}, markedly stimulated the caspase-3 activation, by 11.2 %, 16.4 %, 23.8 %, and 31.5 %, respectively (Fig. 3B).

By the antimicrobial activities of ZnNPs, several studies reported the high efficacy of ZnNPs against a wide range of bacteria, fungi, and virus pathogenic strains, e.g., *Staphylococcus spp., Bacillus spp., Aspergillus spp., Trichophyton spp., Candida spp.,* Hepatitis E virus and Herpes Simplex Virus Type 1 (HSV-1) [14,15]. Concerning the anti-parasitic activities of ZnNPs, in a study conducted by Dkhil et al. [34] reported that five days' treatment with ZnNPs at the dose of 10 mg/kg/day ZNPs, caused a considerable reduction in the oocyst detaching and inflammatory damage in the intestine of mice with *Eimeria papillata* infection. Another investigation by Nazir et al. [35] reported that ZnO meaningfully reduced the viability of *L. tropica* promastigotes with IC_{50} values ranging from 0.012 to 0.084 μg/mL. Jan et al. [36] reported that biogenic synthesis ZnONPs considerably declined the viability of *L. tropica* promastigote and amastigotes with IC_{50} values of 48 μg/mL and 51 μg/mL, respectively. Esmaeilnejad et al. [37], revealed that ZnO NPs at the dose of 16 ppm completely killed the *Haemonchus contortus* helminths followed by 16 h treatment. Reviews reported that ZnNPs perhaps displayed their antimicrobial activities via direct (e.g., affecting on the permeability of cell membrane, cell growth inhibition, and stimulation of apoptosis) and indirect effects (e.g., generating oxidative stress through H_2O_2 creation and release of zinc ions and its entry into the cell and toxic effects on the vital organelles of the cell [38,39]. Considering the cytotoxicity effects of ZnNPs (Suppl.2), the results of the MTT assay of the current investigation showed that the CC_{50} level of the ZnNPs, MA, and ZnNPs + MA was 612.3, 784.6, and 328.4 μg/mL, respectively (Table 2). The calculated SI higher than 10 of ZnNPs alone and in combination with MA displayed the high specificity of ZnNPs to parasites and low toxicity to host cells.

6. Conclusion

Based on these in vitro and in vivo results, green synthesized ZnNPs, mainly along with MA, showed that has the potential to be introduced as a new drug for CL therapy. Triggering of NO production, and inhibition of infectivity rate are revealed as mechanisms of action ZnNPs on *L. major*. But, supplementary investigations are necessary to clear the efficacy and safety of these agents.

CRediT authorship contribution statement

Study design and experiments: **Javad Ghasemian Yadegari**. Data collection: **Mojtaba Shakibaie, and Hamid Reza Mohammadi** Interpretation and data analysis: **Javad Ghasemian Yadegari**, Supervisor: **Hossein Mahmoudvand**. Writing the manuscript draft: **Hossein Mahmoudvand**. Critical revision of the manuscript: **Amal Khudair Khalaf**.

Ethical Statement

The protocols of this investigation are in line with the approvals of the Guide for the Care and Use of Laboratory Animals of the National Institutes of Health; which was agreed upon by the Ethics Committee of the Lorestan University of Medical Sciences, Iran (IR.LUMS.REC.1401.214). This study was carried out in compliance with the ARRIVE guidelines (https://arriveguidelines.org/).

Funding

Not applicable.

Declaration of Competing Interest

The authors declare that they have no known competing financial interests or personal relationships that could have appeared to influence the work reported in this paper.

Availability of Data and Materials

All data generated or analyzed during the present study are included in this published article.

Acknowledgments

The authors would like to thank all people who have contributed to this research.

Consent for publication

Not applicable.

Appendix A. Supporting information

Supplementary data associated with this article can be found in the online version at doi:10.1016/j.biopha.2023.114984.

References

[1] E. Torres-Guerrero, M.R. Quintanilla-Cedillo, J. Ruiz-Esmenjaud, R. Arenas, Leishmaniasis: a review, F1000Research 6 (2017).
[2] B. Alemayehu, M. Alemayehu, Leishmaniasis: a review on parasite, vector and reservoir host, Health Sci. J. 11 (4) (2017) 1.
[3] J. Chakravarty, S. Sundar, Current and emerging medications for the treatment of leishmaniasis, Expert Opin. Pharmacother. 20 (10) (2019) 1251–1265.
[4] S. Sundar, B. Singh, Emerging therapeutic targets for treatment of leishmaniasis, Expert Opin. Ther. Targets 22 (6) (2018) 467–486.
[5] N.K. Copeland, N.E. Aronson, Leishmaniasis: treatment updates and clinical practice guidelines review, Curr. Opin. Infect. Dis. 28 (5) (2015) 426–437.
[6] L.F. Oliveira, A.O. Schubach, M.M. Martins, S.L. Passos, R.V. Oliveira, M. C. Marzochi, C.A. Andrade, Systematic review of the adverse effects of cutaneous leishmaniasis treatment in the New World, Acta Trop. 118 (2) (2011) 87–96.
[7] A. Ponte-Sucre, F. Gamarro, J.C. Dujardin, M.P. Barrett, R. López-Vélez, R. García-Hernández, A.W. Pountain, R. Mwenechanya, B. Papadopoulou, Drug resistance and treatment failure in leishmaniasis: a 21st century challenge, PLoS Negl. Trop. Dis. 11 (12) (2017), e0006052.
[8] A. Nafari, K. Cheraghipour, M. Sepahvand, G. Shahrokhi, E. Gabal, H. Mahmoudvand, Nanoparticles: new agents toward treatment of leishmaniasis, Parasite Epidemiol. Control 10 (2020), e00156.
[9] N. Kulkarni, U. Muddapur, Biosynthesis of metal nanoparticles: a review, J. Nanotechnol. 2014 (2014).

[10] A. Saravanan, P.S. Kumar, S. Karishma, D.V. Vo, S. Jeevanantham, P.R. Yaashikaa, C.S. George, A review on biosynthesis of metal nanoparticles and its environmental applications, Chemosphere 264 (2021), 128580.
[11] N. Roohani, R. Hurrell, R. Kelishadi, R. Schulin, Zinc and its importance for human health: an integrative review, J. Res. Med. Sci.: Off. J. Isfahan Univ. Med. Sci. 18 (2) (2013) 144.
[12] M. Hambidge, Human zinc deficiency, J. Nutr. 130 (5) (2000) 1344S–1349SS.
[13] S. Hojyo, T. Fukada, Roles of zinc signaling in the immune system, J. Immunol. Res. 2016 (2016).
[14] H. Sturikova, O. Krystofova, D. Huska, V. Adam, Zinc, zinc nanoparticles and plants, J. Hazard. Mater. 349 (2018) 101–110.
[15] H. Agarwal, S.V. Kumar, S. Rajeshkumar, A review on green synthesis of zinc oxide nanoparticles–an eco-friendly approach, Resour.-Effic. Technol. 3 (4) (2017) 406–413.
[16] R. Prusinowska, K.B. Śmigielski, Composition, biological properties and therapeutic effects of lavender L). A review, Herba Pol. 60 (2) (2014) 56–66.
[17] H. Mahmoudvand, H.R. Al-Abodi, P. Zolfagharkhani, J. Ghasemian Yadegari, Anti-helminthic effects and cellular mechanisms of Astragalus ecbatanus extract against Echinococcus granulosus protoscoleces, J. Parasit. Dis. 46 (4) (2022) 1047–1054.
[18] V.L. Singleton, R. Orthofer, R.M. Lamuela-Raventós, Analysis of total phenols and other oxidation substrates and antioxidants by means of folin-ciocalteu reagent, Methods Enzym. 299 (1999) 152–178.
[19] N. Phuyal, P.K. Jha, P.P. Raturi, S. Rajbhandary, Total phenolic, flavonoid contents, and antioxidant activities of fruit, seed, and bark extracts of Zanthoxylum armatum DC, Sci. World J. 2020 (2020).
[20] Y. Masoumi-Ardakani, H. Mahmoudvand, A. Mirzaei, K. Esmaeilpour, H. Ghazvini, S. Khalifeh, G. Sepehri, The effect of Elettaria cardamomum extract on anxiety-like behavior in a rat model of post-traumatic stress disorder, Biomed. Pharmacother. 87 (2017) 489–495.
[21] Z. Salari, A. Ameri, H. Forootanfar, M. Adeli-Sardou, M. Jafari, M. Mehrabani, M. Shakibaie, Microwave-assisted biosynthesis of zinc nanoparticles and their cytotoxic and antioxidant activity, J. Trace Elem. Med. Biol. 39 (2017) 116–123.
[22] A.E. Albalawi, A.K. Khalaf, M.S. Alyousif, A.D. Alanazi, P. Baharvand, M. Shakibaie, H. Mahmoudvand, Fe3O4@ piroctone olamine magnetic nanoparticles: synthesize and therapeutic potential in cutaneous leishmaniasis, Biomed. Pharmacother. 139 (2021), 111566.
[23] F.C. Odds, Synergy, antagonism, and what the chequerboard puts between them, J. Antimicrob. Chemother. 52 (2003) 1, https://doi.org/10.1093/jac/dkg301 ([PubMed] [CrossRef] [Google Scholar] [Ref list]).
[24] A.E. Albalawi, S. Abdel-Shafy, A. Khudair Khalaf, A.D. Alanazi, P. Baharvand, K. Ebrahimi, H. Mahmoudvand, Therapeutic potential of green synthesized copper nanoparticles alone or combined with meglumine antimoniate (glucantime®) in cutaneous leishmaniasis, Nanomaterials 11 (4) (2021) 891.
[25] M. Gharavi, M. Nobakht, Sh. Khademvatan, E. Bandani, M. Bakhshayesh, M. Roozbehani, The effect of garlic extract on expression of INFγ and Inos genes in macrophages infected with Leishmania major, Iran. J. Parasitol. 6 (3) (2011) 74–81 (PMID: 22347300; PMCID: PMC3279889).
[26] B. Ezatpour, E. Saedi Dezaki, H. Mahmoudvand, M. Azadpour, F. Ezzatkhah, In vitro and in vivo antileishmanial effects of Pistacia khinjuk against Leishmania tropica and Leishmania major, Evid.-Based Complement. Altern. Med. (2015) 2015.
[27] R.G. Titus, M. Marchand, T. Boon, J.A. Louis, A limiting dilution assay for quantifying L. major in tissues of infected mice, Parasite Immunol. 7 (1985) 545–555.
[28] O. Koushik, Y. Rao, P. Kumar, R. Karthikeyan, Nano drug delivery systems to overcome cancer drug resistance—a review, J. Nanomed. Nanotechnol. 7 (378) (2016) 2.
[29] H. Mahmoudvand, M. Shakibaie, R. Tavakoli, S. Jahanbakhsh, I. Sharifi, In vitro study of leishmanicidal activity of biogenic selenium nanoparticles against Iranian isolate of sensitive and glucantime-resistant Leishmania tropica, Iran. J. Parasitol. 9 (4) (2014) 452.
[30] A.P. Gobert, S. Semballa, S. Daulouede, S. Lesthelle, M. Taxile, B. Veyret, P. Vincendeau, Murine macrophages use oxygen-and nitric oxide-dependent mechanisms to synthesize S-nitroso-albumin and to kill extracellular trypanosomes, Infect. Immun. 66 (9) (1998) 4068–4072.
[31] P. Holzmuller, D. Sereno, M. Cavaleyra, I. Mangot, S. Daulouede, P. Vincendeau, J. L. Lemesre, Nitric oxide-mediated proteasome-dependent oligonucleosomal DNA fragmentation in Leishmania amazonensis amastigotes, Infect. Immun. 70 (7) (2002) 3727–3735, https://doi.org/10.1128/IAI.70.7.3727-3735.2002 (PMID: 12065515; PMCID: PMC128075).
[32] M.A. Savitskaya, G.E. Onishchenko, Mechanisms of apoptosis, Biochemistry 80 (2015) 1393–1405.
[33] N. Van Opdenbosch, M. Lamkanfi, Caspases in cell death, inflammation, and disease, Immunity 50 (6) (2019) 1352–1364.
[34] M.A. Dkhil, S. Al-Quraishy, R. Wahab, Anticoccidial and antioxidant activities of zinc oxide nanoparticles on Eimeria papillata-induced infection in the jejunum, Int. J. Nanomed. 10 (2015) 1961.
[35] S. Nazir, A. Rabbani, K. Mehmood, F. Maqbool, G.M. Shah, M.F. Khan, M. Sajid, Antileishmanial activity and cytotoxicity of ZnO-based nano-formulations, Int. J. Nanomed. 14 (2019) 7809.
[36] H. Jan, M. Shah, H. Usman, M.A. Khan, M. Zia, C. Hano, B.H. Abbasi, Biogenic synthesis and characterization of antimicrobial and antiparasitic zinc oxide (ZnO) nanoparticles using aqueous extracts of the Himalayan Columbine (Aquilegia pubiflora), Front. Mater. 7 (2020) 249.
[37] B. Esmaeilnejad, A. Samiei, Y. Mirzaei, F. Farhang-Pajuh, Assessment of oxidative/nitrosative stress biomarkers and DNA damage in Haemonchus contortus, following exposure to zinc oxide nanoparticles, Acta Parasitol. 63 (3) (2018) 563–571.
[38] K.S. Khashan, G.M. Sulaiman, S.A. Hussain, T.R. Marzoog, M.S. Jabir, Synthesis, characterization and evaluation of anti-bacterial, anti-parasitic and anti-cancer activities of aluminum-doped zinc oxide nanoparticles, J. Inorg. Organomet. Polym. Mater. 30 (9) (2020) 3677–3693.
[39] M. Sasai, A. Pradipta, M. Yamamoto, Host immune responses to Toxoplasma gondii, Int. Immunol. 30 (3) (2018) 113–119.